

# Innovative Thermal and Acoustic Insulation Foams from Recycled Fiberglass Waste

Luca Cozzarini,\* Lucia Marsich, and Alessio Ferluga

This study examines a lightweight thermal and acoustic insulation material, produced starting from a hydrogel-based mixture composed by renewable biopolymer and fiberglass waste powders. The gel 3D porous network is preserved after water removal by sublimation, resulting in a lightweight thermal and acoustic insulation material with good overall performance. Mechanical, thermal, and acoustic properties can be tuned as a function of biopolymer and additives concentration. This material addresses environmental concerns both in terms of secondary raw sources use and fiberglass waste disposal. Moreover, contrary to mineral wools currently on the market, it can overcome the problem of fiber release, with significant human health benefits. Thanks to its good properties and its fabrication process based on a circular economy approach, it can be appealing for thermal and acoustic insulating applications in building and industrial sectors and also in terms of environmental footprint.

## 1. Introduction

Temperature control in buildings and enclosed spaces accounts nowadays for  $\approx 40\%$  of the global energy consumption.<sup>[1–3]</sup> A proper thermal insulation and an improvement in energy efficiency are therefore critical to minimize transmitted heat flow and energy use, thus lowering related emissions.<sup>[4,5]</sup>

The insulating materials market is currently dominated by organic foams (expanded polystyrene and polyurethane foams) and inorganic fibrous materials (glass and mineral wool),<sup>[4,6]</sup> which are commonly used as thermal insulators and soundproofing materials in civil and industrial buildings.<sup>[4,7]</sup> Conventional organic foams are produced from primary raw materials (fossil fuels), while the release of fibers from mineral wool can

raise health concerns.<sup>[8]</sup> Nowadays, in light of an increased awareness of environmental and health issues, there is a strong research interest for substitute materials, aiming at the use of secondary, renewable, or recycled sources to comply with sustainability and ecological requirements.<sup>[5,7]</sup>


Furthermore, the increasing use of fiberglass-reinforced plastics (GFRPs) and other composite material objects (i.e. boats, aircraft, automotive parts, wind turbine blades, etc.) is leading to a growing rate of waste accumulation. Typically, GFRP objects are not easy to recycle, since the thermoset resins composing the material's matrix cannot be easily separated from reinforcing fibers after the curing process. Therefore, their production, use, and end-of-life follow a linear economic

scheme. No cost-effective, environmentally friendly, or practical recycling solutions are available at the moment for these materials. Most of the time, they are simply disposed in landfills; sometimes, to skip disposal cost, they are criminally abandoned in the environment, resulting in pollution and potential health issues due to fibers release. In Europe only,  $\approx 55\,000$  tons of GFRPs are sent to landfill every year<sup>[9,10]</sup>; nevertheless, the European Union set a target to decrease the amount of waste ending up in landfills by 10% by 2030 by adopting innovative recovery/recycling methodologies.<sup>[11]</sup>

The focus of this study is a novel material, produced by a circular economy approach after incorporating fiberglass waste powder within a natural biopolymer matrix, to obtain a foam with good thermal and acoustic insulation properties. To the best of our knowledge, low-temperature production methods without blowing agents are not currently available for this type of materials. The successful production of an open-cell foam produced from natural alginate biopolymer was reported in another work of ours.<sup>[12]</sup> Briefly, the synthesis route is based on the preparation of a hydrogel, which is then freeze-dried; the three-dimensional porous network is preserved after the water entrapped during gelation is removed by sublimation, preventing the pores to collapse. In this study we demonstrate the possibility of including the fiberglass waste as filler inside the biopolymer network; we also tested the addition of plasticizers to tune the mechanical, thermal insulation, and soundproofing properties. This material is capable to addresses both the use of secondary and renewable raw sources and the problem of fiberglass waste disposal/recycling, and it has been proven to be further recyclable itself.<sup>[13]</sup> Moreover, contrary to mineral fiber-based materials currently on the market, this foam overcomes

L. Cozzarini  
Department of Engineering and Architecture  
University of Trieste  
Via Valerio 10, Trieste 34127, Italy  
E-mail: lcozzarini@units.it

L. Marsich, A. Ferluga  
Research & Innovation Department  
MaterialScan Srl.  
Via Capodistria 28, Trieste I-34145, Italy

 The ORCID identification number(s) for the author(s) of this article can be found under <https://doi.org/10.1002/admt.202201953>.

© 2023 The Authors. Advanced Materials Technologies published by Wiley-VCH GmbH. This is an open access article under the terms of the Creative Commons Attribution-NonCommercial License, which permits use, distribution and reproduction in any medium, provided the original work is properly cited and is not used for commercial purposes.

DOI: 10.1002/admt.202201953

the problem of fiber release, with significant environmental and human health benefits. Further details regarding the foam structure, the production process, and its environmental impact are available in our previous works.<sup>[14–17]</sup> Thanks to its good properties and its fabrication process based on a circular economy approach, this innovative material could be appealing for thermal and acoustic insulating applications in building and industrial applications.

## 2. Experimental Section

### 2.1. Samples Production

Alginic acid sodium salt from brown algae (alginate, medium viscosity), glycerol ( $\geq 99.5\%$ ), sorbitol ( $\geq 99.5\%$ ), D-gluconic acid  $\delta$ -lactone (GDL,  $\geq 99.0\%$ ) and calcium carbonate ( $\text{CaCO}_3$ , 98%) were purchased from Sigma Aldrich. Fiberglass scraps (production offcuts) were freely donated by a company in northeastern Italy; scraps were ground by mechanical crusher and ball milling, then screened and sieved to fine powder ( $< 500 \mu\text{m}$ ). Foam production was carried out via a sol-gel process, according to a procedure previously reported.<sup>[12,14]</sup> Briefly, the alginate was mixed with water, fiberglass powder,  $\text{CaCO}_3$ , and GDL (see Table 1 for composition details); the mixture was then poured into  $200 \times 200 \text{ mm}$  molds (gel height was  $\approx 20\text{--}25 \text{ mm}$ ). Samples were left at room temperature for 30 min to complete gelation process; after gelation, they were frozen at  $-20^\circ\text{C}$  for 12 h and finally freeze-dried for 24 h in a 5Pascal LIO5P freeze dryer to remove water. The fiberglass content (weight/volume) was kept constant (12.5% wt./vol.) for all the samples, since it was found, after preliminary tests, to be an optimal compromise between keeping a low density of the sample and maximize its recycled content and mechanical stiffness. Alginate concentration was varied to study their influence on final properties. Glycerol and sorbitol were tested in different concentration and their influence as plasticizers was examined. At least three samples were produced for each composition. After being measured and weighted (see paragraph 2.2.), they were cut into smaller sizes. Square-based samples ( $150 \times 150 \times 15 \text{ mm}$ ) were used for thermal conductivity measurements;  $50 \times 50 \times 15 \text{ mm}$  for mechanical testing and cylindrical samples (diameter 45 mm) for acoustic characterization.

### 2.2. Dimension, Mass, and Density Determination

Before measurements and testing, all samples were conditioned for 24 h at  $20^\circ\text{C}$ , 35% relative humidity. The dimensions

of dried samples were measured with a digital caliper (RS pro, code 841-25), rounding the value to  $10^{-1} \text{ mm}$ , and averaging three measurements for each dimension. The mass was determined with a digital balance (Sartorius CP244S), rounding the value to  $10^{-1} \text{ g}$ , while the volume was calculated as the product of the three dimensions (in the case of square-based samples), or according to  $\pi R^2 H$  (with  $R$  radius and  $H$  height) for cylindrical samples. The density of the samples (rounded value to  $\text{kg m}^{-3}$ ) was calculated by dividing the mass by the volume.

### 2.3. Macro and Micrographs

Sample macroscopic images have been acquired with a digital camera (Panasonic Lumix DMC-TZ80); Scanning Electron Microscopy (SEM) images have been acquired using a SUPRA40 SEM, operating with a 3 kV acceleration voltage with secondary electrons detector.

### 2.4. Mechanical Testing

Compression tests were performed using a Shimadzu AGS-X 10 dynamometer (10 kN load cell). The test speed was set to  $1.3 \text{ mm min}^{-1}$ , while the signal acquisition time was set at 250 msec. Mechanical properties (compression modulus and strength) were determined according to ASTM C165,<sup>[18]</sup> procedure “A” (for samples having an approximate straight-line portion of a load-deformation curve) or procedure “B” (for samples not showing an approximate straight-line portion of a load-deformation curve, that become increasingly stiffer as load is increased). Compression strength was conventionally registered at 10% strain for all samples for comparison purposes.

### 2.5. Thermal Conductivity Determination

The thermal conductivity was measured with a Netzsch HFM 446 heat flow meter on square-based samples ( $150 \times 150 \times 15 \text{ mm}^3$ ) according to the technical standard ASTM C518,<sup>[18]</sup> at an average temperature of  $25^\circ\text{C}$ .

### 2.6. Sound Absorption Measurements

A two-microphone plane wave impedance tube (Kundt's tube) was used to determine the samples' sound absorption properties, according to the ISO 10534-2 standard.<sup>[19]</sup> The noise

**Table 1.** Composition of samples.

Sample nr.	Alginate [wt.%/vol.%]	Fiberglass powder [wt.%/vol.%]	$\text{CaCO}_3$ [wt.%/vol.%]	GDL [wt.%/vol.%]	Plasticizer type	Plasticizer quantity [wt.%/vol.%]	Dry weight [g]
1	2.5	12.5	0.2	1.5	–	–	16.7
2	3.0	12.5	0.2	1.5	–	–	17.2
3	3.5	12.5	0.2	1.5	–	–	17.7
4-9	3.5	12.5	0.2	1.5	glycerol	1 to 5	18.7 – 22.7
10-14	3.5	12.5	0.2	1.5	sorbitol	1 to 5	18.7 – 22.7



**Figure 1.** Representative images of foam samples.

reduction coefficient (NRC) was determined according to the technical standard ASTM C423.<sup>[20]</sup> Three cylindrical samples (diameter 45 mm; thickness 15 mm) were tested for each composition.

### 3. Results and Discussion

#### 3.1. Foam Structure

The principle of the synthesis route is based on the initial formation of a three-dimensional porous hydrogel network, thanks to the crosslink of  $\text{Ca}^{+2}$  ions with G-blocks of the polysaccharide. The slow release of  $\text{Ca}^{+2}$  ions from  $\text{CaCO}_3$  is controlled through the gradual decrease of the pH of the solution due to the GDL hydrolysis in water. This three-dimensional structure is then preserved by freeze-drying, a process that eliminates liquid water and prevents the consequent collapse of pores, leaving a dry, open-porous structure. Macroscopic images of representative samples are shown in **Figure 1**. The open-cell porous structure of the foam can be appreciated in

the representative SEM image reported in **Figure 2**. A more detailed characterization of the cell porosity, performed also by means of X-Ray micro-tomography, is reported in a recent work of ours.<sup>[15]</sup>

#### 3.2. Sample Density

Sample density is reported in **Table 2**. Overall, the densities of our samples lie between 170 and 320  $\text{kg m}^{-3}$ . It is possible to notice that samples with plasticizers are heavier than others; this is most likely due to humidity absorption from atmosphere (even after the conditioning at low humidity for 24h), since both glycerol and sorbitol are hygroscopic molecules.

#### 3.3. Mechanical Properties

Average compression test curves are shown in **Figure 3A–D**. A comparison between samples produced with different concentrations of alginate is shown in **Figure 3A** (labeled Alg 2.5,

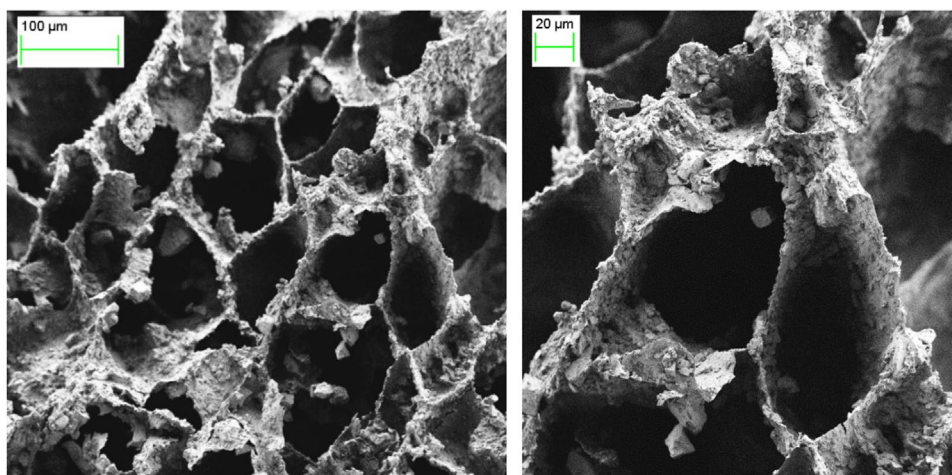


**Figure 2.** Representative SEM images of porous structure.

**Table 2.** Properties of samples.

Alginate [ wt.%/vol%]	Plasticizer [wt.%/vol%]	density	E [GPa]	Compression strength at 10% strain [MPa]	Sound NRC	Thermal conductivity [mW m <sup>-1</sup> K <sup>-1</sup> ]
2.5	–	173 ± 19	3.3 ± 0.3	0.21 ± 0.02	0.25	42 ± 2
3.0	–	177 ± 14	3.2 ± 0.2	0.24 ± 0.01	0.25	45 ± 3
3.5	–	185 ± 12	5.5 ± 0.9	0.32 ± 0.03	0.25	41 ± 2
3.5	glycerol 1.0	207 ± 27	0.86 ± 0.16	0.16 ± 0.02	0.35	66 ± 4
3.5	glycerol 1.5	218 ± 13	0.23 ± 0.02	0.05 ± 0.01	0.40	69 ± 4
3.5	glycerol 5.0	329 ± 30	–	< 0.01	0.45	–
3.5	sorbitol 1.0	203 ± 30	1.11 ± 0.21	0.13 ± 0.02	0.35	56 ± 4
3.5	sorbitol 1.5	217 ± 17	0.98 ± 0.15	0.05 ± 0.01	0.35	61 ± 5
3.5	sorbitol 2.0	240 ± 12	0.64 ± 0.30	0.01 ± 0.00	0.35	65 ± 3
3.5	sorbitol 5.0	322 ± 16	–	< 0.01	0.40	–

3.0, and 3.5, where the number is the alginate concentration expressed as % wt.%/vol.% in the initial aqueous suspension). Similarly, Figure 3B, compares the samples produces with a fixed concentration of alginate (3.5 wt.%/vol.%) and different concentrations of glycerol (1.0, 1.5, and 5.0 wt.%/vol.%). Figure 3C shows the stress-strain curves of samples produces

with a fixed concentration of alginate (3.5 wt.%/vol.%) and different concentrations of sorbitol. The values of compression modulus and compression strength (this latter conventionally registered at 10% strain) are reported in Table 2. Overall, the samples produced without plasticizer show mechanical properties superior to those of average mineral-based insulation

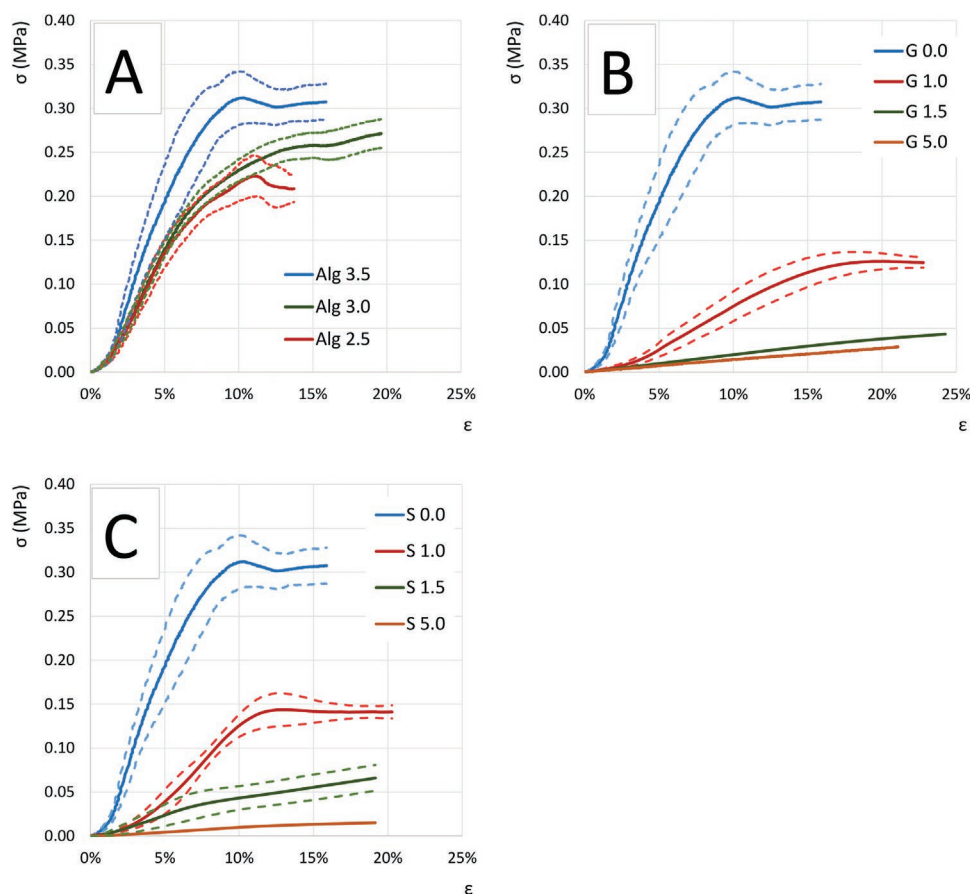


**Figure 3.** Stress/strain compression curves of foam samples. A) comparison between samples produces with different concentrations of alginate (Alg 2.5, 3.0, and 3.5 wt.%/vol.%); B) samples produces with alginate 3.5 wt.%/vol.% and different concentrations of glycerol (G 1.0, 1.5, and 5.0 wt.%/vol.%); C) comparison between samples produces with alginate 3.5 wt.%/vol. and different concentrations of sorbitol (S 1.0, 1.5, and 5.0 wt.%/vol.%).



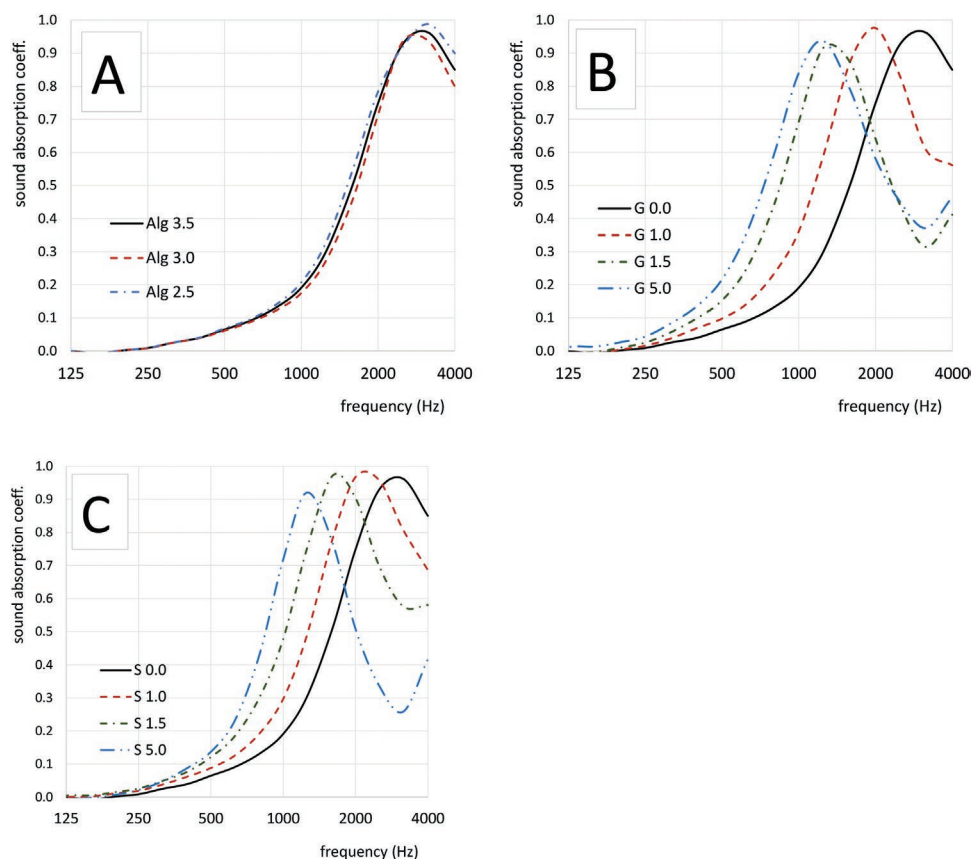


**Figure 4.** Sound absorption coefficient curves of foam samples. A) comparison between samples produces with different concentrations of alginate (Alg 2.5, 3.0, and 3.5 wt.%/vol.); B) samples produces with alginate 3.5 wt.%/vol. and different concentrations of glycerol (G 1.0, 1.5, and 5.0 wt.%/vol.); C) comparison between samples produces with alginate 3.5 wt.%/vol. and different concentrations of sorbitol (S 1.0, 1.5 and 5.0 wt.%/vol.).

materials (glass wool and mineral wool), making them suitable for load-bearing applications. Modulus and compressive strength seem to increase with alginate content, while seem to decrease with the addition of plasticizers, particularly with glycerol. The use of polysaccharides as plasticizers in alginate-based matrix is a well-known practice to reduce their stiffness.<sup>[21–23]</sup> In the works cited above, the authors use higher concentration (up to 5 wt.%/vol.) of glycerol to plasticize nonporous scaffolds. The effect of small amounts of glycerol and sorbitol in our open-cell porous material seems significant in causing a reduction in the foam stiffness. A glycerol concentration of just above 1.5 wt.%/vol. and sorbitol just above 2 wt.%/vol. appears to drastically reduce the modulus and compressive strength.

### 3.4. Sound Absorption Properties

Average curves of noise absorption coefficient as a function of sound frequency are reported in **Figure 4**. Figure 4A shows a comparison between samples produces with different concentrations of alginate (labeled Alg 2.5, 3.0, and 3.5, where the number is the alginate concentration in % wt.%/vol.). Figure 4B similarly, compares the samples produces with a

fixed alginate concentration (3.5 wt.%/vol.) and different concentrations of glycerol (1.0, 1.5, and 5.0 wt.%/vol.). Figure 4C, reports the curves of samples produces with a fixed alginate concentration (3.5 wt.%/vol.) and different concentrations of sorbitol. Values of noise reduction coefficient (NRC) are reported in Table 2. NRC values and overall acoustic performances are better for the plasticized samples: in softer materials, the sound is better absorbed than in stiffer ones, due to the deformation that occurs when the sound wave hits the structure.<sup>[24,25]</sup> The values of NRC are in line or even superior respect to those of commercially available sound-absorbing materials. This can be explained by the low density and the type of porosity. As discussed in other works, the porosity of our foam samples is predominantly open.<sup>[15,26]</sup> With this configuration, the thermal insulation properties are slightly reduced with respect to a closed-pore material but the sound insulation capabilities are improved,<sup>[27]</sup> and this is well reflected by the good soundproofing performances recorded. Varying the alginate concentration between 2.5 and 3.5 wt.%/vol. does not seem to affect the sound absorption properties, while the addition of plasticizing molecules (glycerol and sorbitol) seems to shift the absorption maximum to lower frequencies and improve the overall NRC values, most likely due to the softening of the structure.

### 3.5. Thermal Insulation Properties

Values of thermal conductivity (reported in Table 2) lie between 41 and 65 mW m<sup>-1</sup> K<sup>-1</sup>. They appear to be only loosely related to the density of the samples (with heavier ones showing higher conductivities). Variation in alginate concentration does not seem to affect thermal conductivity, while plasticizers concentration appears to negatively affect the thermal insulation properties, likely due to water absorption. For comparison, rock wool, glass wool, expanded polystyrene, or polyurethane foam perform slightly better (20–30 mW m<sup>-1</sup> K<sup>-1</sup>) with respect to our samples.<sup>[4,6,28,29]</sup> Reasonably, thermal conductivity is influenced by density and porosity structure (closed cells favor thermal insulation). The conduction in the solid phase (related to the density of the sample) contributes more to the overall thermal conductivity, while conduction in the gas phase is greater in an open-cell structure due to convective heat transfer.<sup>[27]</sup> Our open-cell structure, alongside a higher density with respect to expanded polymeric foams, hinders optimal heat-insulation performances.

## 4. Conclusions

The results showed that it is possible to produce a lightweight thermal and acoustic insulation material starting from a renewable biopolymer and GFRP waste. This novel material shows an open porous structure, with density between 170 and 320 kg m<sup>-3</sup>, thermal conductivities between 35 and 65 mW m<sup>-1</sup> K<sup>-1</sup>, a noise-reducing factor of 0.25–0.45 and compressive strengths as high as 0.3 MPa, making it an interesting candidate for applications which require a good combination of low weight, thermal/acoustic insulation and a minimal amount of mechanical strength. Although thermal insulation performances are not outstanding when compared to polymeric foams, the soundproofing performances and load-bearing capacity can exceed those of mineral wools with similar density. Moreover, preliminary results show that most of these properties can be finely tuned by varying the concentration of the biopolymer and/or by adding polysaccharides as plasticizers. Finally, benefits in terms of environmental indices and life cycle analysis are evident. Life Cycle Analysis approach will assume a significant value in the next future and a manufacturing process able to reduce energy consumption, raw material use, dust, fibers, and CO<sub>2</sub> emissions will be strategic. Our production method starts from secondary raw materials, limiting the energy required with respect to that necessary to extract, transport, and process primary raw materials which are often used for the production of other insulating foams. Furthermore, instead of sending composite materials waste to landfill, this process will recycle them into a nearly state-of-the-art insulating foam. From preliminary tests outcomes, our innovative foams have similar insulating properties to average mineral wool (50 mW m<sup>-1</sup> K<sup>-1</sup>). Therefore we will be able to offer a product with similar properties to those already on the market, but with environmental advantages (carbon footprint reduction and sustainability) respect to traditional insulators. In terms of resource efficiency, this will avoid the production of new organic foams or mineral wool, saving raw materials, energy and limiting CO<sub>2</sub> emission in the atmos-

phere. Also, public health will be improved, since fiber release from the foam is limited and only additives from natural origin are used.

## Acknowledgements

This work was supported by “GGTDoors – Green Gas Tight Doors” project funded by Regione Autonoma Friuli Venezia Giulia, POR-FESR 2014–2020.

Open access funding provided by Università degli Studi di Trieste within the CRUI-CARE agreement.

## Conflict of Interest

The authors declare no conflict of interest.

## Data Availability Statement

The data that support the findings of this study are available from the corresponding author upon reasonable request.

## Keywords

thermal insulating materials, soundproofing, fiberglass recycling, biopolymers, circular economy

Received: November 16, 2022

Revised: February 20, 2023

Published online: March 19, 2023

- [1] European Commission, Energy efficiency in buildings, <https://ec.europa.eu/info/news/focus-energy-efficiency-buildings-2020-lut-17>, (accessed: October 2022).
- [2] US Dept. of Energy, Building Energy Data Book, <https://openet.org/doe-opendata/dataset/6aaf0248-bc4e-4a33-9735-2babe-4aef2a5/resource/3edf59d2-32be-458b-bd4c-796b3e14bc65/download/2011bedb.pdf> (accessed: October 2022).
- [3] UN Environ. Program, Sustainable Buildings and Climate Initiative, <https://www.unenvironment.org/explore-topics/resource-efficiency/what-we-do/cities/sustainable-buildings> (accessed: October 2022).
- [4] S. Schiavoni, F. D'Alessandro, F. Bianchi, F. Asdrubali, *Renewable Sustainable Energy Rev.* **2016**, 62, 988.
- [5] F. Asdrubali, F. D'Alessandro, S. Schiavoni, *Sustainable Mater. Technol.* **2015**, 4, 1.
- [6] B. Abu-Jdayil, A.-H. Mourad, W. Hittini, M. Hassan, S. Hameedi, *Constr. Build. Mater.* **2019**, 214, 709.
- [7] A. M. Papadopoulos, E. Giam, *Build. Environ.* **2007**, 42, 2178.
- [8] P. Harrison, P. Holmes, R. Bevan, K. Kamps, L. Levy, H. Greim, *Regul. Toxicol. Pharmacol.* **2007**, 73, 425.
- [9] D. E. Witten, V. Mathes, The Market for Glass Fibre Reinforced Plastics (GRP) in 2020, <https://eucia.eu/userfiles/files/AVK%20Market%20Report%202020.pdf> (accessed: October 2022).
- [10] D. Arabsolgar, A. Musumeci, in *The 8th Annual International Sustainable Places Conference (SP2020) Proceedings*, MDPI (Multidisciplinary Digital Publishing Institute), Basel, Switzerland **2021**, p. 23.
- [11] European Commission, Closing the loop – An EU action plan for the circular economy, <https://www.eea.europa.eu/policy-documents/com-2015-0614-final> (accessed: October 2022).

- [12] G. Kyawoo D'amore, M. Caniato, C. Schmid, L. Marsich, A. Ferluga, L. Cozzarini, A. Marinò, *Technol. Sci. Ships Future* **2018**, <https://doi.org/10.3233/978-1-61499-870-9-332>.
- [13] M. Cibinel, G. Pugliese, D. Porrelli, L. Marsich, V. Lughi, *Carbohydr. Polym.* **2021**, 251, 116995.
- [14] L. Cozzarini, L. Marsich, A. Ferluga, C. Schmid, *Developments in the Built Environment* **2020**, 3, 100014.
- [15] M. Caniato, L. Cozzarini, C. Schmid, A. Gasparella, *Sustainable Mater. Technol.* **2021**, 28, e00274.
- [16] A. Mio, S. Bertagna, L. Cozzarini, E. Laurini, V. Bucci, A. Marinò, M. Fermeglia, *Sustainable Mater. Technol.* **2021**, 29, e00327.
- [17] A. Kumar, D. Naumenko, L. Cozzarini, L. Barba, A. Cassetta, M. Pedio, *J. Raman Spectrosc.* **2018**, 49, 1015.
- [18] "ASTM C165-07 - Standard Test Method for Measuring Compressive Properties of Thermal Insulations", American Society for Testing and Materials, <https://www.astm.org/c0165-07r17.html>.
- [19] "ISO 10534-2:1998 - Acoustics — Determination of sound absorption coefficient and impedance in impedance tubes — Part 2: Transfer-function method", International Organization for Standardization, <https://www.iso.org/standard/22851.html>.
- [20] "ASTM C423-22 - Standard Test Method for Sound Absorption and Sound Absorption Coefficients by the Reverberation Room Method", American Society for Testing and Materials, <https://www.astm.org/c0423-22.html>.
- [21] S. Gao, Y. Zeng, *J. Appl. Polym. Sci.* **1993**, 47, 2065.
- [22] G. I. Olivas, G. V. Barbosa-Cánovas, *LWT – Food Science and Technology* **2008**, 41, 359.
- [23] A. Travan, F. Scognamiglio, M. Borgogna, E. Marsich, I. Donati, L. Tarusha, M. Grassi, S. Paoletti, *Carbohydr. Polym.* **2016**, 150, 408.
- [24] J. Allard, N. Atalla, *Propagation of Sound in Porous Media: Modelling Sound Absorbing Materials*, Wiley, Hoboken, N.J. **2009**.
- [25] M. A. Shaid Sujon, A. Islam, V. K. Nadimpalli, *Polym. Test.* **2021**, 104, 107388.
- [26] M. Caniato, L. Cozzarini, C. Schmid, A. Gasparella, *Sci. Rep.* **2022**, 12, 10955.
- [27] J. P. Holman, *Heat Transfer*, McGraw-Hill Education, Boston **2012**.
- [28] ASTM International, Standard, Specification for Rigid, Cellular Polystyrene Thermal Insulation (ASTM C578-18).
- [29] ASTM International, Standard Specification for Spray-Applied Rigid Cellular Polyurethane Thermal Insulation (ASTM C1029-20).